Enhancing Road Holding and Vehicle Comfort for an Active Suspension System utilizing Model Predictive Control and Deep Learning

Do Trong Tu
Mechanical and Power Engineering Faculty, Electric Power University, Vietnam
tudt@epu.edu.vn (corresponding author)

Received: 1 November 2023 | Revised: 27 November 2023 and 19 December 2023 | Accepted: 31 December 2023

 DOI: https://doi.org/10.48084/etasr.6582

ABSTRACT

Active Suspension Systems (ASS) with control are gaining traction as researchers strive for optimal system performance. They are significant in diverse commercial vehicle applications, catering to user demands. This study employs the advanced Model Predictive Control (MPC) technique to enhance the smoothness and safety of a half-car model. The simulation results showed the prowess of MPC controllers under varied control force signal constraints, demonstrating superiority in curtailing vehicle chassis rotation angle and speed by up to 46.93% and 43.34%, respectively. The controller was compared with an artificial neural network controller utilizing only two state signals of the system, trained from MPC data, demonstrating high accuracy with R^2 reaching 0.97024 and mean squared error at 7.3557×10^{-5}. This study contributes to the refinement of ASS by focusing on practical implementation and performance enhancement.

Keywords-active suspension system; model predictive control; machine learning; deep learning; artificial neural networks; ride comfort; road holding

I. INTRODUCTION

Active Suspension Systems (ASSs) enhance ride comfort, handling, and vehicle stability by dynamically adjusting components, counteracting chassis roll, and optimizing tire contact with the road. ASSs in vehicles use advanced control strategies such as Proportional-Integral-Derivative (PID), Fuzzy Logic Network (FLC), and Linear Quadratic Regulator (LQR) controllers to enhance system criteria. A PID controller uses error feedback to adjust damping forces and maintain the desired suspension response [1]. FLC can use linguistic variables to handle uncertainties and variations in road conditions [2], ensuring smoother ride adaptability. LQR controllers optimize a quadratic cost function to balance ride comfort and stability [3]. These control techniques enable an ASS to continuously adapt and respond to changing road conditions, ensuring optimal performance and safety while providing passengers with a comfortable and controlled ride experience. However, conventional controllers have limited adaptability, struggle with complex systems, and require manual tuning, whereas Model Predictive Control (MPC) offers advanced control capabilities and robustness for complex multivariable systems. This technique is highly effective, seamlessly accommodates system nonlinearities, and excels in diverse applications across industries due to its ability to handle MIMO formulations, various physical restrictions, and multiple objectives [4]. Several studies investigated active suspension system control strategies in automobiles using ISO-based road characteristics [5-7]. According to these simulations, MPC greatly improves suspension performance and power demand compared to LQR [8-9]. Semi-active vibration control suspension systems use magnetorheological dampers to improve automobile dynamics [10], specifically the quarter vehicle's with semi-active suspension [11-15]. In [16], constrained MPC formulation for longitudinal control and a nonlinear MPC reduced computing cost. In [17], a Particle Swarm-Optimization Model Predictive Controller (PSO-MPC) was used to determine the best control actions. In [14], an explicit MPC approach was presented to supervise the damping force in semi-active vehicle suspensions, and an AFC-based scheme was proposed to control active seat suspension in heavy-duty vehicles. In [18], Parallel Quadratic Programming (PQR), an iterative multiplication technique, was used to address quadratic programming issues in a real-time MPC model. In [19], the focus was on generalization, active suspension test benches, and stability and robustness conditions.

An Artificial Neural Network (ANN) is a powerful and adaptive approach that can be applied effectively to improve the performance of ASSs in vehicles by learning from real-time sensor data and intelligently adjusting suspension components. It effectively models complex relationships and improves ride comfort, stability, and safety, reducing body roll, pitch, and squat during maneuvers [20]. The multifaceted PSO approach has been applied on quarter-car thorax and pelvis models, demonstrating zero head acceleration, low sprung mass acceleration, and equivalent road-holding qualities. In [21-22], ANN models were constructed to accurately predict road holding and ride comfort characteristics. Novel methods have

been proposed for the development of automobile chassis systems that approximate the correlations between design factors and performance indices. In [23], the minimal sensitivity approach was used to generate Pareto-optimal alternatives and evaluate their robustness. Several simulations showed that the B-spline neural network trajectory tracking control architecture is capable of active disturbance suppression [24-25], indicating that ANN, FLC, LQR, and PID controllers are all capable of active disturbance suppression. In [26], an intelligent control strategy for active truck suspensions based on ANNs was presented, with the control arm of the Macpherson suspension system being critical for a comfortable, stable, and safe ride. In [27], a low-cost semi-active car suspension system was presented, with a hydraulic piston and throttle valve replacing passive conventional suspension. In [28], an ANN control technique was used for continuous damping control dampers in car suspension systems to decrease the positional oscillation in road imperfections. In [29], PSO was used for parameter optimization, showing an 84% decrease in iteration resources and a 48% improvement in modeling accuracy for hydraulic adjustable dampers.

II. DESIGN CONTROLLERS FOR HALF-CAR MODEL

A. Vehicle Dynamic Modeling

Figure 1 presents a half-car model with 6 degrees of freedom, simplified with the dynamics equations around the equilibrium as follows:

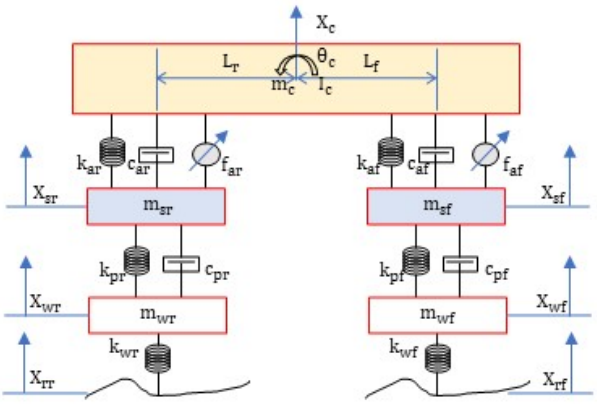

Fig. 1. Half-car model with ASS.

$$\ddot{X}_c = -\frac{c_{af}}{m_c} L_f \dot{\theta}_c \cos\Theta_c - \frac{c_{af}}{m_c}\dot{X}_c - \frac{c_{af}}{m_c}\dot{X}_{sf} - \frac{k_{af}}{m_c} L_f \sin\Theta_c - \frac{k_{ar}}{m_c} X_c + \frac{k_{ar}}{m_c} X_{sf} + \frac{1}{m_c} f_{af} + \frac{c_{ar}}{m_c} L_r \dot{\theta}_c \cos\Theta_c - \frac{c_{ar}}{m_c}\dot{X}_c + \frac{c_{ar}}{m_c}\dot{X}_{sr} + \frac{k_{af}}{m_c} L_r \sin\Theta_c - \frac{k_{ar}}{m_c} X_c + \frac{k_{ar}}{m_c} X_{sr} + \frac{1}{m_c} f_{ar} \quad (1)$$

$$\ddot{\Theta}_c = -L_f^2 \frac{c_{af}}{I_c}\dot{\theta}_c \cos\Theta_c - L_f \frac{c_{af}}{I_c}\dot{X}_c + L_f \frac{c_{af}}{I_c}\dot{X}_{sf} - L_f^2 \frac{k_{af}}{I_c} \sin\Theta_c + L_f \frac{k_{af}}{I_c} X_{wf} - L_f \frac{k_{af}}{I_c} X_c + \frac{L_f}{I_c} f_{af} - L_r^2 \frac{c_{ar}}{I_c}\dot{\theta}_c \cos\Theta_c + L_r \frac{cr}{I_c}\dot{X}_c - L_r \frac{c_{ar}}{I_c}\dot{X}_{wr} - L_r^2 \frac{k_{ar}}{I_c} \sin\Theta_c + L_r \frac{k_{ar}}{I_c} X_{wr} - L_r \frac{k_{ar}}{I_c} X_{wr} + \frac{L_r}{I_c} f_{ar} \quad (2)$$

$$\ddot{X}_{sr} = -\frac{c_{ar}}{m_{sr}} L_r \dot{\theta}_c \cos\Theta_c + \frac{c_{ar}}{m_{sr}}\dot{X}_c - \frac{c_{ar}}{m_{sr}}\dot{X}_{sr} - \frac{k_{ar}}{m_{sr}} L_r \sin\Theta_c + \frac{k_{ar}}{m_{sr}} X_c - \frac{k_{ar}}{m_{sr}} X_{sr} - \frac{c_{pr}}{m_{sr}}\dot{X}_{sr} + \frac{c_{pr}}{m_{sr}}\dot{X}_{wr} - \frac{k_{pr}}{m_{sr}} X_{sr} + \frac{k_{pr}}{m_{sr}} X_{wr} - \frac{1}{m_{sr}} f_{ar} \quad (3)$$

$$\ddot{X}_{sf} = \frac{c_{af}}{m_{sr}} L_f \dot{\theta}_c \cos\Theta_c + \frac{c_{af}}{m_{sf}}\dot{X}_c - \frac{c_{af}}{m_{sf}}\dot{X}_{sf} + \frac{k_{af}}{m_{sf}} L_f \sin\Theta_c + \frac{k_{af}}{m_{sf}} X_c - \frac{k_{af}}{m_{sf}} X_{sf} - \frac{k_{pf}}{m_{sf}} X_{sf} + \frac{kf}{m_{sf}} X_{wf} - \frac{c_{pf}}{m_{sf}}\dot{X}_{sf} + \frac{c_{pf}}{m_{sf}}\dot{X}_{wf} - \frac{1}{m_{sf}} f_{af} \quad (4)$$

$$\ddot{X}_{wf} = \frac{c_{pf}}{m_{wf}}\dot{X}_{sf} - \frac{c_{pf}}{m_{wf}}\dot{X}_{wf} + \frac{k_{pf}}{m_{wf}} X_{sf} - \frac{k_{pr}}{m_{wf}} X_{wf} - \frac{k_{wf}}{m_{wf}} X_{wf} + \frac{k_{wf}}{m_{wf}} X_{rf} \quad (5)$$

$$\ddot{X}_{wr} = \frac{c_{pr}}{m_{wr}}\dot{X}_{sr} - \frac{c_{pr}}{m_{wr}}\dot{X}_{wr} + \frac{k_{pr}}{m_{wr}} X_{sr} - \frac{k_{pr}}{m_{wr}} X_{wr} - \frac{k_{wr}}{m_{wr}} X_{wr} + \frac{k_{wr}}{m_{wr}} X_{rr} \quad (6)$$

B. Model Predictive Control for Active Suspension System

The MPC algorithm revolves around iteratively solving an optimization problem at every time interval. The primary objective is determining the optimal control inputs that minimize a predefined cost function, ensuring adherence to system dynamics and constraints across a finite prediction horizon. This optimization process can be succinctly represented in the following manner:

1) Objective Function

The proposed model seeks to minimize road hold and comfort criteria for the half-car model. The objective function, also known as the cost function, quantifies system performance based on predicted system states and control inputs. This function defines the goal of the control problem and can be customized to meet specific requirements. The general form of the cost function is:

$$J = \sum[q(x_k, u_k) + \mathrm{r}(u_k)] \quad (8)$$

where J is the total cost over the prediction horizon, $q(x_k, u_k)$ is the state cost with a function of the predicted system states x_k and control inputs u_k at time step k, and $r(u_k)$ is the control cost which consists of a function of the control inputs at time step k.

2) System Dynamics

The system dynamics, shown in Figure 2, are described by a discrete-time model predicting state evolution over time based on the current state x_k and control inputs u_k:

$$x_{k+1} = f(x_k, u_k) \quad (8)$$

where $x_{(k+1)}$ is the predicted state at the next time step (k+1), and f is the state transition function that describes how the state evolves based on the current state and control input.

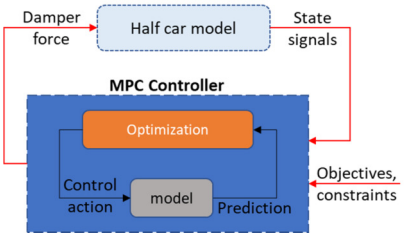

Fig. 2. MPC architecture.

3) Constraints

The constraint is to limit the range of allowed controlled force values to ASS to absorb the external vibration from the road transferred to the vehicle. The constraints are defined as follows:

$$g(x_k, u_k) \leq 0 \quad h(x_k) = 0 \tag{9}$$

where $g(x_k, u_k)$ is a vector of inequality constraint functions on the states and control inputs, and $h(x_k)$ is a vector of inequality constraint functions on the states.

4) Optimization Problem

MPC aims to find the optimal control inputs that minimize the cost function subject to the system dynamics and constraints over the prediction horizon. The optimization problem is formulated as follows:

$$\begin{aligned} \text{minimize } J &= \sum[q(x_k, u_k) + r(u_k)] \\ x_{k+1} &= \mathrm{f}(x_k, u_k) \\ \text{subject to } \quad \mathrm{g}(x_k, u_k) &\leq 0 \\ h(x_k) &= 0 \end{aligned} \tag{10}$$

The optimization problem is solved each time step, taking the current state of the system as an initial condition. The first control input from the optimal solution is involved in the system, and the procedure is repeated in the subsequent step, effectively employing the receding horizon control. For these proposed MPC models, the Sequential Quadratic Programming (SQP) optimizer is used to define optimal control inputs. It approximates nonlinear problems with quadratic subproblems, linearizing the cost function and constraints at each step to update control input u_k. The process involves iteratively solving these subproblems, aiming to converge to optimal control inputs that satisfy system dynamics and constraints, ultimately enhancing the MPC's ability to handle nonlinear and constrained optimization tasks.

C. Artificial Neural Network for Active Suspension System

A standard ANN architecture for predicting dampers' acting force includes input layers, interconnected hidden layers, and an output layer, is shown in Figure 3. Input features x_t at a given time encompass relevant information, including past observations from the half-car model with signals θ_c and $\dot{\theta}_c$. These features are split into training, testing, and validation sets (70-20-10) by trial-and-error, transforming weighted connections and activation functions in hidden layers to make predictions. The outputs of the 10 hidden layers at time t are expressed by:

$$h_t^l = \sigma(W_l h_{t-1}^{l-1} + b_l) \tag{11}$$

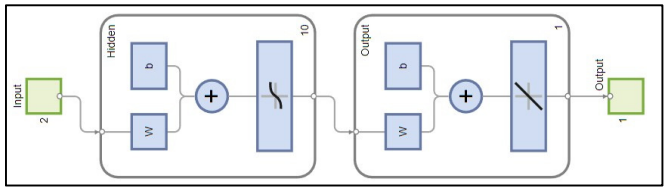

Fig. 3. Construction of ANN controller for ASS.

In (11), h_t^l signifies the output of the l^{th} hidden layer at time t, W_l denotes the weight matrix governing the connections, h_{t-1}^{l-1} represents the prior hidden layer's output at time t-1, b_l is the bias vector, and σ corresponds to the sigmoid activation function. The ultimate output prediction $\hat{y}_{t+1}$ is obtained by applying the final hidden layer's output to the output layer to observe the acting force F_{af} and F_{ar} at ASS for the half-car:

$$\hat{y}_{t+1} = W_o h_n^t + b_o \tag{12}$$

where W_o stands for the weight matrix associated with the output layer, h_n^t denotes the last hidden layer's output at time t, and b_o represents the bias term.

$$MSE = \frac{1}{N}\sum_{i=1}^{N}(y_i - \hat{y}_i) \tag{13}$$

$$R^2 = 1 - \frac{\sum_{i=1}^{N}(y_i - \hat{y}_i)^2}{\sum_{i=1}^{N}(y_i - \bar{y})^2} \tag{14}$$

where N is the number of samples, y_i is the actual target value of the i^{th} sample, $\hat{y}_i$ is the predicted target value of the i^{th} sample, and $\bar{y}$ is the mean of the target values. The parameters of the neural network, which include weights and biases, are iteratively adjusted through the Bayesian regularization backpropagation algorithm. This process aims to minimize the disparity between the network's predicted value $\hat{y}_{t+1}$ and the actual observed value y_{t+1}. The model refines its weights and biases through 156 successive iterations to enhance its predictive accuracy by the Mean Squared Error (MSE) (13) at 7.3557×10^{-5} and R^2 = 0.97024 (14). Their ASS characteristics are shown in Figure 4. Figure 4(c) shows the error histogram of the ANN controller, demonstrating the distribution of errors between predicted and actual values within the model performance context. On the horizontal axis, various ranges are displayed, while the vertical axis indicates the frequency of data points within each error interval. This analysis highlights that the error parameters related to the prediction of the ASS control force fall mostly within the approximately ± 45 N range. This alignment with the prescribed constraints of the mechanism strongly validates the feasibility of the proposed approach.

III. SIMULATION RESULTS AND ANALYSIS

To assess and simulate the efficacy of the controllers in the context of the ASS applied to a half-car model, the exogenous

disturbance signals originating from the road profile were assumed to be discretized step functions within the simulated time domain. The computer configuration used in the computation was an Intel® Core™ i7-11700F 64GB RAM, NVIDIA GeForce 3080 RTX that trained ANN in 20 min. This modeling approach allows for the analysis of controller performance under realistic road conditions, as expressed by:

$$X_{rf}(t) = \begin{cases} 0 & if\ t < 1 \\ 0.1.e^{t-1} & if\ t \geq 1 \end{cases}$$
$$X_{rr}(t) = \begin{cases} 0 & if\ t < 1 + delay \\ 0.1.e^{t-1-delay} & if\ t \geq 1 + delay \end{cases} \quad (15)$$

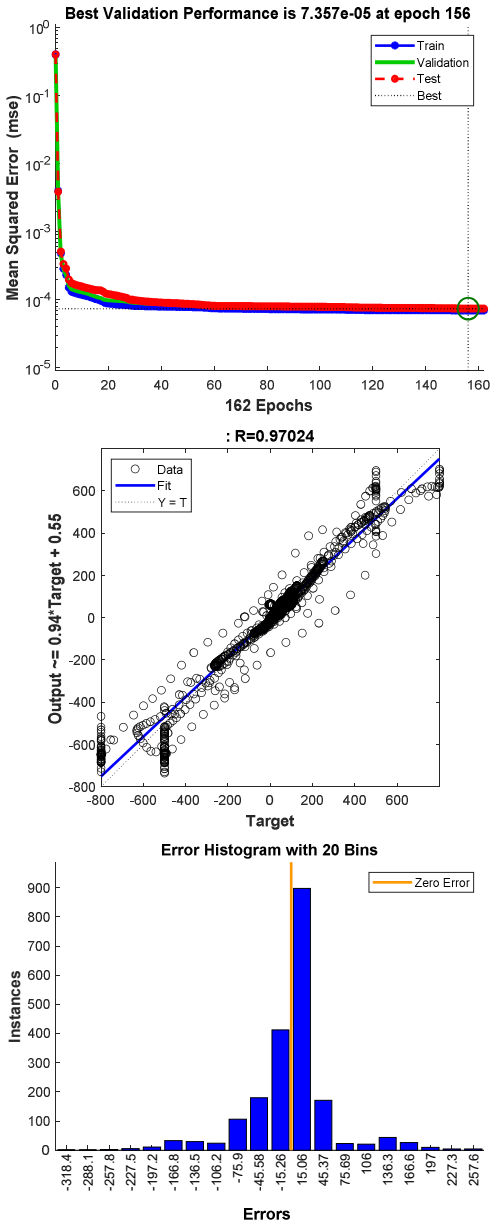

Fig. 4. (a) MSE, (b) linear regression, and (c) error histogram of the ANN model.

Figure 5 shows the simulation results of the suggested models under the influence of step pavement profile excitation, with a rate of 1 s applied to the front suspension, 0.4 s to the rear suspension, and valued at 0.1 m. The MPC model with a control force limit of 2000 N is represented by the red dotted line, while the MPC0 model, constrained to a control force of 1500 N, is depicted by the blue dashed line. The solid black line with star remarks depicts the results achieved through the passive suspension model, while the green solid line denotes the results achieved using the ANN controller.

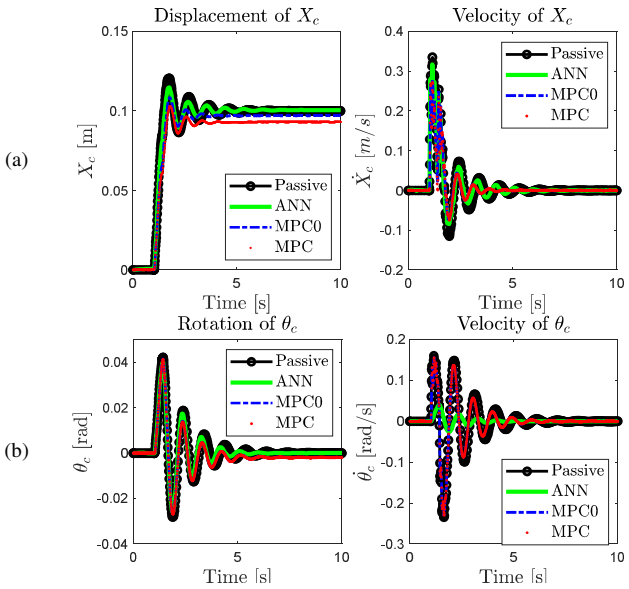

Fig. 5. Time response of chassis with exogenous disturbance: (a) Displacement of chassis and its velocity due to time simulation, (b) Comparing the chassis rotation and its velocity under different controllers.

Figure 5(a) shows a comparison of the chassis attributes, contrasting the use of the ASS system with MPC and ANN controllers against the passive suspension model. It is evident that by increasing the constraint on the damping control force, the performance of the MPC controller within the ASS model exceeds that of the MPC0 controller. Specifically, the reduction in chassis speed is notable, with a decrease of 46% and 43% for the MPC and MPC0 controllers, respectively, compared to the passive suspension model. Figure 5(b) shows that when employing the ANN controller in the ASS system, a notable reduction of 8.82% was achieved in the angular velocity of the chassis, in stark comparison to the results exhibited by the passive suspension model. Table I details the amplitude reduction in the Root Mean Squared (RMS) values of the signals compared to the passive suspension model.

The control forces employed in the ASS models are showcased, contributing to the refinement of the proposed model's smoothness and traction. In response to stepwise excitation, controllers generate damping control forces to mitigate detrimental vibrations that impact both the vehicle and its occupants. These force magnitudes are strategically determined to fulfill the criteria established for the constraint conditions of the model, guided by the MPC control algorithm.

The MPC0 controller adheres to a control force threshold of 1500 N, while the MPC controller adheres to a limit of 2000 N, as in [30-31]. The passive suspension model entirely depends on traditional dampers lacking actuators, leading to a simulation with a control force of 0 N. Figure 5 shows the RMS error values for the X_c, $\dot{X}_c$, Θ_c and $\dot{\Theta}_c$ of the models. These observations reveal that the proposed suite of controllers significantly contributes to advancing the controller's initial objectives: vehicle comfort and road holding. Notably, the RMS signals of the system employing the ANN controller exhibit the most substantial reduction, succeeded by the MPC controller and, ultimately, the MPC0 controller. Therefore, in an ideal scenario, the ANN controller optimally utilizes only two measured sensor inputs, namely Θ_c and $\dot{\Theta}_c$, harnessing the acquired intelligence from the ASS model. This approach effectively minimizes the sensor system expenses for the ASS system while simultaneously maintaining the predetermined objectives with a high precision level.

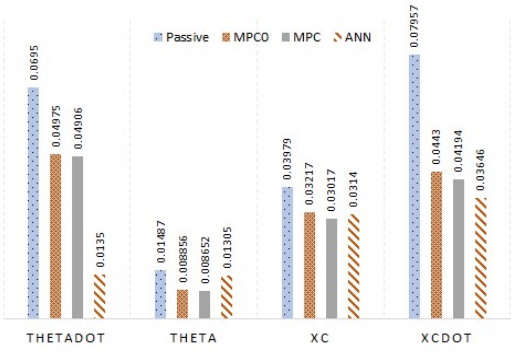

Fig. 6. RMS values of $\dot{\Theta}_c$,Θ_c,X_c, and $\dot{X}_c$.

TABLE I. RMS REDUCTION OF FRONT/REAR WHEELS AND INTERMEDIATE MASSES (%)

Model	X_{sr}	$\dot{X}_{sr}$	X_{wr}	$\dot{X}_{wr}$	X_{sf}	$\dot{X}_{sf}$	X_{wf}	$\dot{X}_{wf}$
MPC0	14.24	36.07	12.79	43.17	11.32	46.93	4.86	42.02
MPC	14.38	36.18	12.84	43.34	11.24	45.82	5.4	41.04
ANN	11.05	26.97	3.42	4.17	8.77	6.01	0.54	4.99

IV. CONCLUSION

This study aimed to improve vehicle movement smoothness and safety using MPC controllers for a half-car model. The controllers demonstrated adaptability to different conditions, reducing chassis rotation by 46%. The ANN controller was effective in training the ASS system with limited states, achieving an R^2 of 0.97024 and an MSE of 7.3557×10^{-5}. However, directly measuring idealized states can be challenging, prompting future investigations into state estimation algorithms. The study lays the groundwork for exploring deep learning models with unsupervised algorithms, enhancing MPC models for accuracy in uncertain settings, and conducting real-world experiments with disturbances and uncertainties.

REFERENCES

[1] P. Gandhi, S. Adarsh, and K. I. Ramachandran, "Performance Analysis of Half Car Suspension Model with 4 DOF using PID, LQR, FUZZY and ANFIS Controllers," *Procedia Computer Science*, vol. 115, pp. 2–13, Jan. 2017, https://doi.org/10.1016/j.procs.2017.09.070.

[2] M. G. Unguritu, T. C. Nichițelea, and D. Selișteanu, "Design and Performance Assessment of Adaptive Harmonic Control for a Half-Car Active Suspension System," *Complexity*, vol. 2022, Jul. 2022, Art. no. e3190520, https://doi.org/10.1155/2022/3190520.

[3] P. Swethamarai and P. Lakshmi, "Adaptive-Fuzzy Fractional Order PID Controller-Based Active Suspension for Vibration Control," *IETE Journal of Research*, vol. 68, no. 5, pp. 3487–3502, Sep. 2022, https://doi.org/10.1080/03772063.2020.1768906.

[4] M. Al-Ashmori and X. Wang, "A Systematic Literature Review of Various Control Techniques for Active Seat Suspension Systems," *Applied Sciences*, vol. 10, no. 3, Jan. 2020, Art. no. 1148, https://doi.org/10.3390/app10031148.

[5] M. Gohari and M. Tahmasebi, "Active Off-Road Seat Suspension System Using Intelligent Active Force Control," *Journal of Low Frequency Noise, Vibration and Active Control*, vol. 34, no. 4, pp. 475–489, Dec. 2015, https://doi.org/10.1260/0263-0923.34.4.475.

[6] V. Deshpande and Y. Zhang, "Multivariable Receding Horizon Control of Aircraft with Actuator Constraints," in *2020 IEEE International Conference on Systems, Man, and Cybernetics (SMC)*, Toronto, ON, Canada, Jul. 2020, pp. 1846–1851, https://doi.org/10.1109/SMC42975.2020.9282815.

[7] J. Kim, T. Lee, C. J. Kim, and K. Yi, "Model predictive control of a semi-active suspension with a shift delay compensation using preview road information," *Control Engineering Practice*, vol. 137, Aug. 2023, Art. no. 105584, https://doi.org/10.1016/j.conengprac.2023.105584.

[8] J. Narayan, S. A. Gorji, and M. M. Ektesabi, "Power reduction for an active suspension system in a quarter car model using MPC," in *2020 IEEE International Conference on Energy Internet (ICEI)*, Sydney, NSW, Australia, Dec. 2020, pp. 140–146, https://doi.org/10.1109/ICEI49372.2020.00033.

[9] D. Rodriguez-Guevara, A. Favela-Contreras, F. Beltran-Carbajal, D. Sotelo, and C. Sotelo, "Active Suspension Control Using an MPC-LQR-LPV Controller with Attraction Sets and Quadratic Stability Conditions," *Mathematics*, vol. 9, no. 20, Jan. 2021, Art. no. 2533, https://doi.org/10.3390/math9202533.

[10] A. S. Gad, "Preview Model Predictive Control Controller for Magnetorheological Damper of Semi-Active Suspension to Improve Both Ride and Handling," *SAE International Journal of Vehicle Dynamics, Stability, and NVH*, vol. 4, no. 3, pp. 305–326, Sep. 2020, https://doi.org/10.4271/10-04-03-0021.

[11] J. Narayan, S. A. Gorji, and M. M. Ektesabi, "Force Optimization for an Active Suspension System in a Quarter Car Model Using MPC," in *Advances in Industrial Machines and Mechanisms*, 2021, pp. 459–474, https://doi.org/10.1007/978-981-16-1769-0_42.

[12] V. N. Mai, D. S. Yoon, S. B. Choi, and G. W. Kim, "Explicit model predictive control of semi-active suspension systems with magneto-rheological dampers subject to input constraints," *Journal of Intelligent Material Systems and Structures*, vol. 31, no. 9, pp. 1157–1170, May 2020, https://doi.org/10.1177/1045389X20914404.

[13] W. Jia, W. Zhang, F. Ma, and L. Wu, "Attitude Control of Vehicle Based on Series Active Suspensions," *Actuators*, vol. 12, no. 2, Feb. 2023, Art. no. 67, https://doi.org/10.3390/act12020067.

[14] Z. Houzhong, L. Jiasheng, Y. Chaochun, S. Xiaoqiang, and C. Yingfeng, "Application of explicit model predictive control to a vehicle semi-active suspension system," *Journal of Low Frequency Noise, Vibration and Active Control*, vol. 39, no. 3, pp. 772–786, Sep. 2020, https://doi.org/10.1177/1461348418822170.

[15] M. Papadimitrakis and A. Alexandridis, "Active vehicle suspension control using road preview model predictive control and radial basis function networks," *Applied Soft Computing*, vol. 120, May 2022, Art. no. 108646, https://doi.org/10.1016/j.asoc.2022.108646.

[16] K. Chen, Z. Li, W. C. Tai, K. Wu, and Y. Wang, "MPC-based Vibration Control and Energy Harvesting Using an Electromagnetic Vibration Absorber With Inertia Nonlinearity," in *2020 American Control Conference (ACC)*, Denver, CO, USA, Jul. 2020, pp. 3071–3076, https://doi.org/10.23919/ACC45564.2020.9147503.

[17] J. O. Pedro, S. M. S. Nhlapo, and L. J. Mpanza, "Model Predictive Control of Half-Car Active Suspension Systems Using Particle Swarm Optimisation," *IFAC-PapersOnLine*, vol. 53, no. 2, pp. 14438–14443, Jan. 2020, https://doi.org/10.1016/j.ifacol.2020.12.1443.

[18] M. Brand *et al.*, "A Parallel Quadratic Programming Algorithm for Model Predictive Control," *IFAC Proceedings Volumes*, vol. 44, no. 1, pp. 1031–1039, Jan. 2011, https://doi.org/10.3182/20110828-6-IT-1002.03222.

[19] D. Rodriguez-Guevara, A. Favela-Contreras, F. Beltran-Carbajal, C. Sotelo, and D. Sotelo, "A Differential Flatness-Based Model Predictive Control Strategy for a Nonlinear Quarter-Car Active Suspension System," *Mathematics*, vol. 11, no. 4, Jan. 2023, Art. no. 1067, https://doi.org/10.3390/math11041067.

[20] B. Zaparoli Cunha, C. Droz, A. M. Zine, S. Foulard, and M. Ichchou, "A review of machine learning methods applied to structural dynamics and vibroacoustic," *Mechanical Systems and Signal Processing*, vol. 200, Oct. 2023, Art. no. 110535, https://doi.org/10.1016/j.ymssp.2023.110535.

[21] J. Niresh, N. Archana, and G. Anand Raj, "Optimisation of Linear Passive Suspension System Using MOPSO and Design of Predictive Tool with Artificial Neural Network," *Studies in Informatics and Control*, vol. 28, no. 1, pp. 105–110, Mar. 2019, https://doi.org/10.24846/v28i1y201911.

[22] M. P. Nagarkar, M. A. El-Gohary, Y. J. Bhalerao, G. J. Vikhe Patil, and R. N. Zaware Patil, "Artificial neural network predication and validation of optimum suspension parameters of a passive suspension system," *SN Applied Sciences*, vol. 1, no. 6, May 2019, Art. no. 569, https://doi.org/10.1007/s42452-019-0550-0.

[23] M. G. Pisino Giampiero Mastinu, Carlo Doniselli, Luca Guglielmetto, Enrico, "Optimal & Robust Design of a Road Vehicle Suspension System," in *The Dynamics of Vehicles on Roads and on Tracks*, Boca Raton, FL, USA: CRC Press, 2000.

[24] F. Beltran-Carbajal, H. Yañez-Badillo, R. Tapia-Olvera, J. C. Rosas-Caro, C. Sotelo, and D. Sotelo, "Neural Network Trajectory Tracking Control on Electromagnetic Suspension Systems," *Mathematics*, vol. 11, no. 10, Jan. 2023, Art. no. 2272, https://doi.org/10.3390/math11102272.

[25] A. Bataineh, W. Batayneh, and M. Okour, "Intelligent Control Strategies for Three Degree of Freedom Active Suspension System," *International Review of Automatic Control (IREACO)*, vol. 14, no. 1, Jan. 2021, Art. no. 17, https://doi.org/10.15866/ireaco.v14i1.20057.

[26] A. Hamza and N. Ben Yahia, "Heavy trucks with intelligent control of active suspension based on artificial neural networks," *Proceedings of the Institution of Mechanical Engineers, Part I: Journal of Systems and Control Engineering*, vol. 235, no. 6, pp. 952–969, Jul. 2021, https://doi.org/10.1177/0959651820958516.

[27] M. Ghoniem, T. Awad, and O. Mokhiamar, "Control of a new low-cost semi-active vehicle suspension system using artificial neural networks," *Alexandria Engineering Journal*, vol. 59, no. 5, pp. 4013–4025, Oct. 2020, https://doi.org/10.1016/j.aej.2020.07.007.

[28] Z. Ding, F. Zhao, Y. Qin, and C. Tan, "Adaptive neural network control for semi-active vehicle suspensions," *Journal of Vibroengineering*, vol. 19, no. 4, pp. 2654–2669, Jun. 2017, https://doi.org/10.21595/jve.2017.18045.

[29] J. Lin, H. Li, Y. Huang, Z. Huang, and Z. Luo, "Adaptive Artificial Neural Network Surrogate Model of Nonlinear Hydraulic Adjustable Damper for Automotive Semi-Active Suspension System," *IEEE Access*, vol. 8, pp. 118673–118686, 2020, https://doi.org/10.1109/ACCESS.2020.3004886.

[30] G. N. Sahu, S. Singh, A. Singh, and M. Law, "Static and Dynamic Characterization and Control of a High-Performance Electro-Hydraulic Actuator," *Actuators*, vol. 9, no. 2, Jun. 2020, Art. no. 46, https://doi.org/10.3390/act9020046.

[31] G. Yang and J. Yao, "Multilayer neuroadaptive force control of electro-hydraulic load simulators with uncertainty rejection," *Applied Soft Computing*, vol. 130, Nov. 2022, Art. no. 109672, https://doi.org/10.1016/j.asoc.2022.109672.